C. R. Physique 16 (2015) 168–181

Contents lists available at ScienceDirect

Comptes Rendus Physique

www.sciencedirect.com

Multiferroic materials and heterostructures / Matériaux et hétérostructures multiferroïques

Artificial multiferroic heterostructures for an electric control of magnetic properties

Hétérostructures multiferroïques artificielles pour un contrôle électrique des propriétés magnétiques

Vincent Garcia, Manuel Bibes, Agnès Barthélémy

Unité mixte de physique CNRS/Thales, campus de l'École polytechnique, 1, avenue Augustin-Fresnel, 91767 Palaiseau, France

ARTICLE INFO

Article history:
Available online 19 February 2015

Keywords:
Multiferroics
Heterostructures
Magnetoelectric coupling
Interfaces
Spintronics
Ferroelectrics

Mots-clés :
Multiferroïques
Hétérostructures
Couplage magnétoélectrique
Interfaces
Spintronique
Ferroélectriques

ABSTRACT

The control of magnetism by electric fields is an important goal for future low-power spintronics devices. This partly explains the intensified recent interest for magnetoelectric multiferroic materials and heterostructures. The lack of ferro- or ferrimagnetic–ferroelectric materials with large magnetoelectric coupling between the two orders has spurred intensive research on artificial multiferroics combining ferroelectric or piezoelectric materials and ferromagnets. In this paper we review synthetically the potential of thin-film-based heterostructures in which a magnetic film is in contact with a ferroelectric or piezoelectric one to obtain an electric control of magnetic properties. This electric control either results from a strain-induced magnetoelectric coupling, a charge-driven one, or from the modulation of an interfacial exchange-bias interaction.

RÉSUMÉ

Contrôler électriquement les propriétés magnétiques des matériaux et réaliser ainsi de nouveaux composants faiblement consommateurs en énergie est un des enjeux de la future électronique de spin. Ceci explique l'intérêt considérable porté aux matériaux et architectures multiferroïques. Malgré des recherches intenses, le graal d'un composé à la fois ferroélectrique et ferro- ou ferrimagnétique à température ambiante avec un fort couplage magnétoélectrique entre ces deux propriétés n'a pas encore été trouvé. Pour pallier ce manque, de nombreux travaux ont porté sur les multiferroïques artificiels, hétérostructures combinant un matériau ferroélectrique ou piézoélectrique et un composé ferromagnétique. Cet article constitue une revue succincte du potentiel de ces hétéro-structures en géométrie planaire pour obtenir un contrôle électrique des propriétés magnétiques. Un tel contrôle peut être obtenu par un effet magnétoélectrique indirect basé sur un couplage d'origine élastique, de façon directe par une modulation des charges dans le ferromagnétique induite par la ferroélectricité ou encore en exploitant le couplage d'échange à l'interface entre un multiferroïque et un matériau magnétique.

E-mail address: agnes.barthelemy@thalesgroup.com (A. Barthélémy).

http://dx.doi.org/10.1016/j.crhy.2015.01.007
1631-0705/

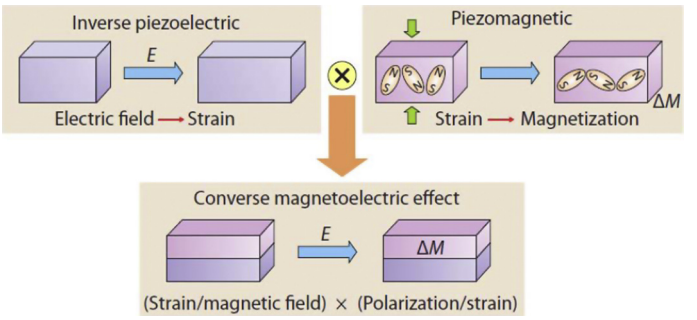

Fig. 1. (Color online.) Schematic illustration of strain mediated converse magnetoelectric coupling. An electric field induces strain on the ferroelectric material which is mechanically transferred to the magnetic material leading changes in the magnetization via the piezomagnetic effect [11].

Multiferroic materials [1], after almost 40 years of hibernation, have been subject of a renewed interest in the early 2000s [2,3]. In particular magnetoelectric multiferroics presenting coupled magnetic and ferroelectric order parameters have attracted a lot of attention. From a fundamental point of view since magnetism and ferroelectricity tends to exclude each other [4], new paths have to be found to stabilize both coupled orders in the same compound. Another attractive trait of these materials is their potential applications for the next generation of electronic devices based on the control of the magnetic state by an electric field and vice versa. Such multifunctional materials could be used in solid-state transformers, magnetic field sensors or actuators. In the particular field of spintronics, they should enable a local control of magnetization to design electrically writable non-volatile magnetic memories with low-power consumption. Despite an intense activity in the field, the grail of a ferromagnetic–ferroelectric multiferroic with large magnetoelectric (ME) coupling at room temperature has not yet been found [3]. This scarcity of room temperature multiferroics with large ME coupling has spurred intensive research on composite multiferroics combining ferroelectric (FE) or piezoelectric materials and ferromagnets (FMs). These two-phase compounds have been elaborated as nanoparticles of one compound embedded in a matrix of the other compound, vertical nanopillar-based heterostructures or multilayers. Good reviews on the subject can be found in references [5–8]. Here, we will focus synthetically on the third geometry, i.e. on thin-film-based heterostructures in which a magnetic film is in contact with a FE or piezoelectric one. We will show how the electric control of magnetic properties can be achieved in such heterostructures—more extensive reviews can be found in references [9] and [10]. This electric control either results from a strain-induced ME coupling, a charge-driven ME effect, or a modulation of the interfacial exchange-bias interaction.

1. Strain-mediated magnetoelectric multiferroics

In strain-mediated magnetoelectric multiferroics (Fig. 1), when a magnetic film is in contact with a ferroelectric one, an external electric field yields a change in the size of the FE lattice parameter through the converse piezoelectric effect. The resulting strain induced on the magnetic material in contact, changes its magnetic properties notably its anisotropy by magnetostriction. The corresponding converse ME coupling thus results from the product of the magnetostrictive effect in the magnetic phase and the piezoelectric effect in the FE one. It is defined as [8,12]:

$$\text{Converse ME effect} = \frac{\text{Mechanical}}{\text{Electric}} \times \frac{\text{Magnetic}}{\text{Mechanical}} = \text{piezoelectric} \times \text{magnetostrictive}$$

$$\Delta M = \alpha \Delta E$$

This mechanism allows us to obtain a ME coupling, defined by the α coefficient, by far larger than in single-phase multiferroics in which it is limited by the square root of the product of the magnetic and electric susceptibilities [2]. This ME coupling has been observed in a large number of systems, unfortunately, it does not generally produce two different magnetic states at electrical remanence. Indeed, the voltage dependence of the magnetic properties reflects that of the strain, as evidenced by the electric field dependence of the strain and magnetization presented in Fig. 2A and B [13].

In heterostructures combining a FE with large piezoelectric coefficients with a soft FM, large magnetostatic energy can be generated by modest voltages which results in a control of its magnetic anisotropy, i.e., its magnetization easy axis. Pertsev [16] used a phenomenological approach to predict an abrupt (progressive) rotation of $CoFe_2O_4$ (Ni) easy-axis magnetization from in-plane to out-of-plane, and vice versa, in heterostructures combining these magnetic materials with $PbZn_{1/3}Nb_{2/3}O_3$–$PbTiO_3$ (PZN–PT) or $PbMg_{1/3}Nb_{2/3}O_3PbTiO_3$ (PMN–PT) ferroelectric relaxors. Hu and Nan [17] confirmed these predictions, extended the study to other combinations of FE ($BaTiO_3$ (BTO), PbZrTiO3 (PZT)) and FM (Fe, Fe_3O_4) materials, and discussed the possibility of an in-plane reorientation of the magnetization.

From an experimental point of view, most effort has been devoted to the combination of a FM, from either the transition metal or oxide families with BTO, PMN–PT or PZN–PT materials. For FM materials grown on BTO substrates, several groups reported the observation of jumps or kinks in the temperature dependence of the magnetization (see an example in Fig. 2C)

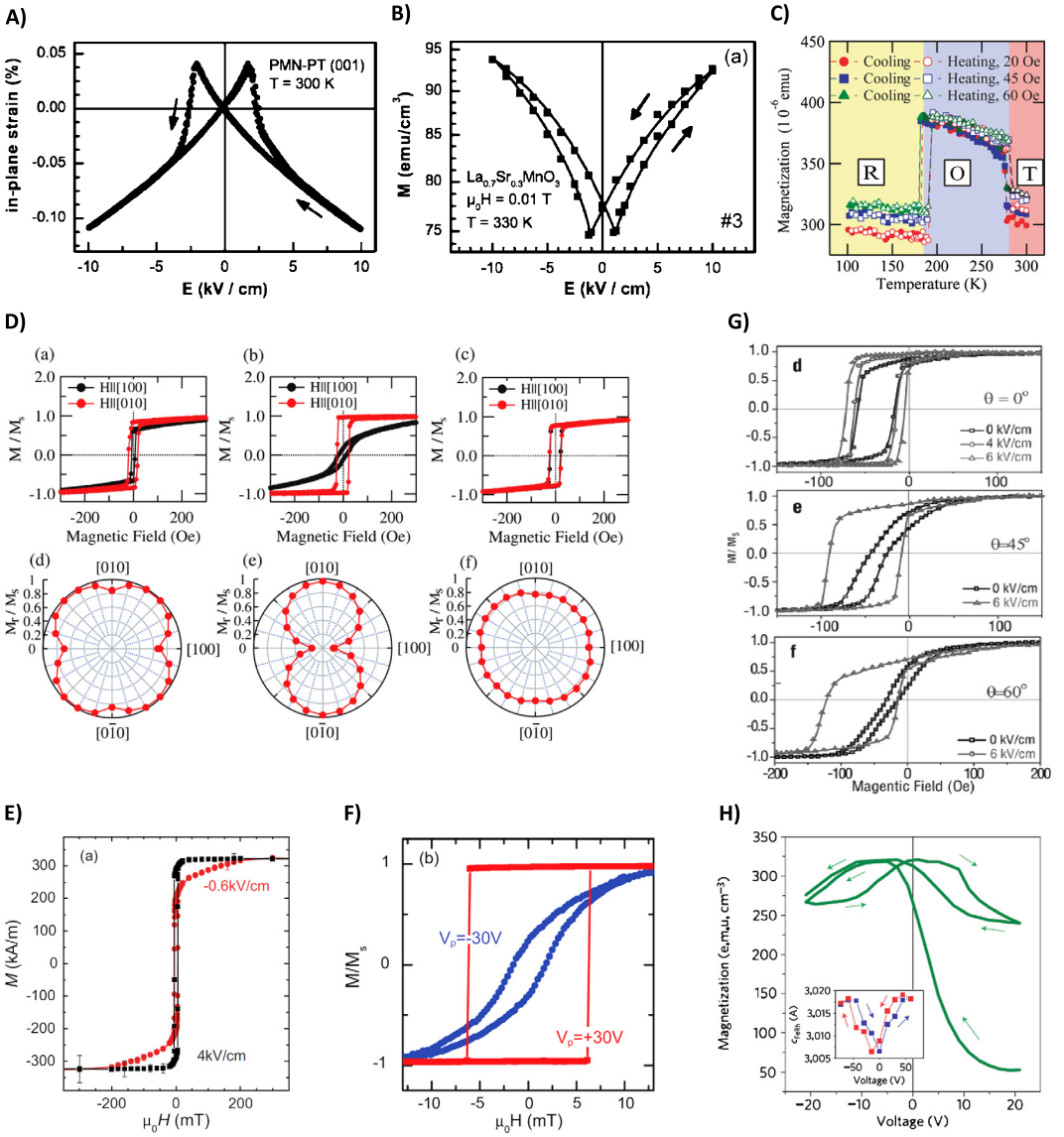

Fig. 2. (Color online.) A) In-plane piezoelectric strain versus applied electric field of a $Pb(Mg_{1/3}Nb_{2/3})_{0.72}Ti_{0.28}O_3$ (PMN–PT) substrate [13]. B) Magnetization M vs. electric field E curve for a field applied to the PMN–PT substrate of $La_{0.7}Sr_{0.3}MnO_3$/PMN–PT heterostructures [13]. C) Temperature dependence of the magnetization of a Fe layer grown on $BaTiO_3$ (BTO) substrates, in magnetic fields of 20, 45 and 60 Oe along [100]. The letters R, O and T represent the rhombohedral, orthorhombic and tetragonal phases of BTO respectively [14]. D) Top: normalized magnetization curves of a Fe/BTO heterostructure for a magnetic field applied along the [100] (black) and [010] (red) directions at (a) room temperature, (b) 230 K, and (c) 150 K. Bottom: polar plots of the normalized remanent magnetization (M_r/M_s) at (d) room temperature (T phase), (e) 230 K (O phase), and (f) 150 K (R phase) [15]. E) In-plane magnetic hysteresis loops $M(H)$ of Ni films for different electric fields applied across the BTO substrate at room temperature [27]. F) In-plane magnetization versus electric field of Ni films deposited on $Pb(Zr,Ti)O_3$ (PZT)-based actuators, for two different voltages V_P applied across the actuator. For $V_P = 30$ V, a rectangular shape is observed characteristic of a magnetic easy axis along the applied field, while for $V_P = -30$ V, the s-shaped loop reflects a hard axis magnetization direction [29]. G) Strain-mediated E-field control of exchange bias due to the competition between exchange-bias-induced unidirectional anisotropy and strain-dependent uniaxial anisotropy in $FeMn/Ni_{80}Fe_{20}$/FeGaB/PZT(011) heterostructures. θ is the angle between the applied magnetic field and the magnetization easy axis [01–1]. From [30]. H) Variation of the magnetization with the electric field of a $Fe_{0.5}Rh_{0.5}$ film deposited on a BTO substrate. The electric field applied across the substrate progressively drives a transformation from a mixed state of a- and c-type ferroelectric domains to a homogeneous c-state (inset) [48].

at the temperatures corresponding to the structural transition temperature of BTO (see for instance references [14,18–23] and [24]). This behavior reflects changes in the magnetic anisotropies induced by the different strain states imposed by the phases of BTO (as evidenced by the polar plot of the remanent magnetization presented in Fig. 2D). Thus, it evidences an efficient elastic coupling between the FM film and the substrate.

A resulting strain-mediated electric control of the magnetic properties has been reported in systems combining ferrites, manganites, transition metals and alloys, or Terfenol-D ($Tb_{1-x}Dy_xFe_2$) as FM compounds and BTO, PZT, PMN–PT, PZN–PT,

$BiScO_3$–$PbTiO_3$ or polyvinylidene fluoride (PVDF) as ferroelectric materials. In some cases, this strain-mediated mechanism was assisted by a charge-mediated mechanism [25,26].

To reveal the efficiency of this converse magnetoelectric coupling, a simple method consists in measuring the magnetization versus magnetic field loops with a vibrating sample magnetometer, SQUID or Kerr effect, while applying an electric field. Prototypical examples corresponding to the electrical control of the magnetic state of Ni are presented in Fig. 2E and F. In the case of Ni deposited on BTO substrate shown in Fig. 2E, the decrease of the electric field from +4 kV/cm to −0.6 kV/cm induced a change of the ferroelectric domain configuration from a single c-domain state (out-of-plane polarization) to a mixed a- (in-plane polarization) and c-domain configuration [27]. This modification corresponds to two different strain states and consequently modifies the magnetic anisotropy resulting in two different values of the magnetization at magnetic remanence and saturation field. Larger effects have been observed in PZT-based actuators combined with Ni film [28,29]. An illustration is given in Fig. 2F. The rectangular to s-like variation in the shape of the magnetic hysteresis loop reveals the rotation of the magnetization while changing the voltage applied to the PZT actuator from +30 V to −30 V [29]. In these experiments, the magnetic easy axis of the Ni film rotated reversibly by 55° at room temperature. Liu et al. observed the strain-mediated control of the magnetization of a FeMn/NiFe/FeGaB trilayer deposited on a PZN–PT(011) substrate due to the elastic tuning of the uniaxial anisotropy of the NiFe/FeGaB bilayer in competition with unidirectional anisotropy due to exchange bias at the NiFe/FeMn interface (Fig. 2G) [30]. They also reported on a nearly 180° deterministic magnetization switching induced in these heterostructures under the application of an electric field at suitable angle and a small additional magnetic field.

Interestingly, whereas the strain vs electric field butterfly loop shows no remanence when the applied electric field range overcomes the coercive field, a remanent strain can be obtained for a smaller range of electric field and could be exploited to obtain a bistable magnetization state [29,31].

An alternative way to probe the change in magnetic anisotropy while varying the strain induced by different ferroelectric configurations is to measure the shift of the ferromagnetic resonance (FMR) signal under the electric field. For example, in FeGaB/PZN–PT heterostructure, a large electric (E)-field-induced change in the FMR spectra (with a FMR field shift of about 750 Oe) was evidenced by Lou et al. and associated with the large *E*-field-induced strain tuning of the magnetic anisotropy [32]. Similar results were reported for other systems with an 860 Oe FMR shift in Fe_3O_4/PZN–PT ([33]) and up to 3500 Oe in Terfenol/PZN–PT heterostructures [34].

Another approach to evidence magnetoelectric coupling is to show the correlation between ferroelectric domains and magnetic ones. This may be achieved either by using optical microscopy (birefringent contrast revealing ferroelectric domains while magneto-optical Kerr contrast allows to image ferromagnetic domains), or by combining magnetic force microscopy (MFM), Lorentz force microscopy or X-ray magnetic circular dichroism photoelectron microscopy (XMCD-PEEM) and X-ray linear dichroism photoelectron microscopy (XLD-PEEM) or piezoresponse force microscopy (PFM) to image ferromagnetic and ferroelectric domains respectively. For example, Chung et al. evidenced the *E*-field-induced change in the ferromagnetic domain configuration of a Ni film deposited on a PZT film sandwiched between two conductive Pt electrodes by MFM (Fig. 3A) [35]. More recently, Lahtinen et al. demonstrated the ferroelectric-to–ferromagnetic pattern transfer of a $BaTiO_3$ substrate in a thin CoFe film by optical microscopy as presented in Fig. 3B [36,37]. The ferroelastic *a*1–*a*2 domain structure consists of stripes wherein the elongation of the unit cell is in the substrate plane. It induces a uniaxial lattice strain and thus magnetoelastic anisotropy in the overlaying CoFe film. The 90° rotation of the elongated *c* axis at the domain boundaries realigns the uniaxial magnetoelastic anisotropy axis and results in a modulation of the magnetization direction of the ferromagnetic film (see Fig. 3B, a and b). Application of a perpendicular electric field ($E = 10$ kV/cm) transforms the ferroelectric microstructure into alternating *a*1 and *c* domains with in-plane and out-of-plane polarization, respectively (see Fig. 3B, c). These ferroelastic modifications are accompanied by changes in the local strain, which is transferred to the CoFe film, and in turn, results in the erasure (on top of *a*1 domains) and conservation (on top of *c* domains) of the original ferromagnetic stripe pattern (Fig. 3B, d). Similarly, Chopdekar et al. evidenced that at room temperature, the *c*-axis-oriented BTO domain, which has its ferroelectric axis along the surface normal, yields a fourfold symmetric strain state in the epitaxial film, whereas the *a*-axis-oriented BTO domain, whose ferroelectric axis lies within the plane of the substrate, yields a twofold symmetric strain state in the film [38]. By changing the orientation of the ferroelectric axis of domains in the BTO substrate via temperature cycling, they evidenced a variation in the magnitude and symmetry of the film strain and the corresponding large changes in the magnetic anisotropy of $CoFe_2O_4$ and $NiFe_2O_4$ thin films on top [38]. Interestingly, it was predicted that the abrupt rotation of the ferroelectric polarization at FE domain walls (DWs) and the concurrent instant change of magnetic anisotropy in the adjacent FM strongly pins the magnetic DWs onto their ferroelectric counterparts. This pinning between magnetic and FE DWs allows us to drag the magnetic DWs when an applied electric field moves the FE ones at a time-averaged velocity equal to the FE DW velocity [39], which is promising for future magnetic memories [40] and logic devices [41].

The *E*-field control of the magnetic properties via strain effects is more complex in manganites. In this case, changes induced in the magnetic and transport properties are related to the modification of the Mn–O–Mn bond angle and bond lengths under piezoelectric strain. A strain-mediated modulation of the magnetization or/and Curie temperature has been reported for $La_{1-x}Sr_xMnO_3$ [13,18,19,42–44], $La_{1-x}Ca_xMnO_3$ [13,45], $La_{0.875}Ba_{0.125}MnO_3$ [46] and $Pr_{0.6}Ca_{0.4}MnO_3$ [47] films deposited on BTO or PMN–PT substrates. Notably, Thiele et al. reported an *E*-field-induced 25% modulation of the magnetization of $La_{0.7}Sr_{0.3}MnO_3$ films at 330 K (see Fig. 2B) that perfectly mimics the strain response. A large change in the Curie temperature (19K) was also reported [13]. Eerenstein et al. observed similar effects for $La_{0.7}Sr_{0.3}MnO_3$ films on

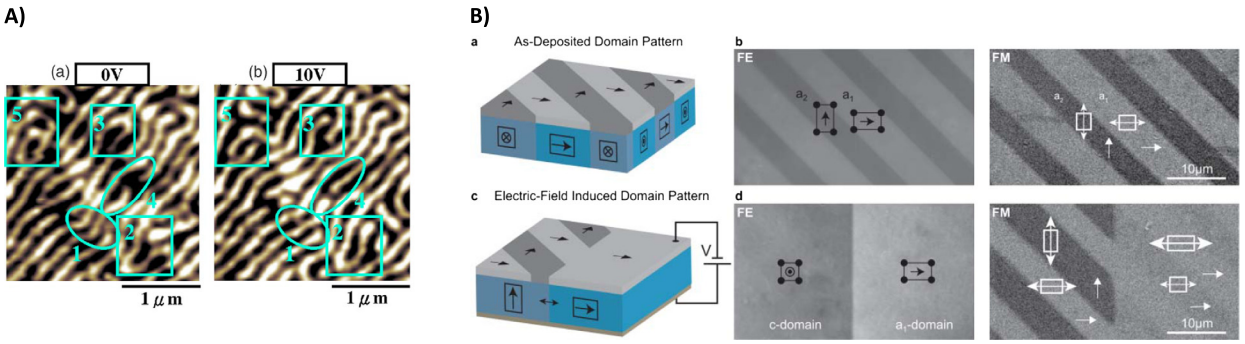

Fig. 3. (Color online.) A) E-field-induced change in the magnetic domain pattern of a Ni film deposited on PZT revealed by MFM. Two different ferromagnetic domain configurations are observed at 0 V (a) and 10 V (b) [35]. B) Ferroelectric (left) and magnetic (right) domain pattern of a CoFe/BTO multiferroic heterostructure imaged by optical polarization microscopy. The $a1/a2$ ferroelectric domain stripe pattern of the BTO substrate (a) induces a uniaxial magnetoelastic anisotropy that rotates by 90° from one domain to another (b) (black arrows indicate the direction of the ferroelectric polarization; white arrows indicate the orientation of the strain-induced magnetic easy axis). The out-of-plane (10 kV/cm) electric field turns the $a2/a1$ ferroelectric domain configuration into a $c/a1$ one (c) and results in a local 90° rotation of the magnetization (d) [37].

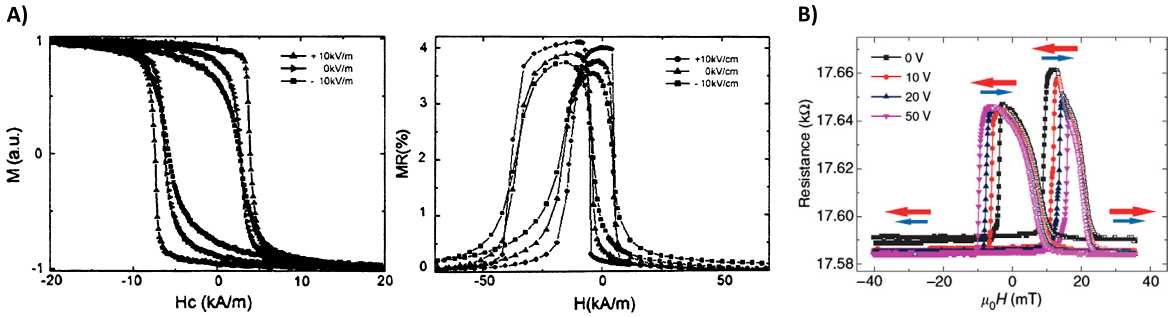

Fig. 4. (Color online.) A) Magnetization versus magnetic field (left) and GMR (right) of an IrMn/$Co_{50}Fe_{50}$/Cu/$Co_{50}Fe_{50}$ spin valve upon application of a voltage to the PZT substrate. The strain changes the anisotropy of the $Co_{50}Fe_{50}$ free layer, resulting in a change of the coercive field [52]. B) GMR of a CoFeB/Cu/Co/IrMn spin valve on PZT for different voltages applied to the substrate. The change reflects the large increase in the coercive field of the CoFeB free layer under stress [53].

BTO substrates and reported sharp and persistent changes in the magnetization when an electric field was applied [19], corresponding to a ME coefficient of up to 2.3×10^{-7} s m^{-1}. In the case of $Pr_{0.6}Ca_{0.4}MnO_3$, Chen et al. reported a 60% enhancement of the magnetization at low temperature under the application of an electric field to the PMN–PT substrate, which was attributed to the E-field-induced change in the phase separation of this magnetic compound [47].

Recently, this strain strategy has been applied to tune the magnetism of $Fe_{0.5}Rh_{0.5}$ films deposited on BTO substrates close to room temperature [48]. At equiatomic composition, $Fe_{0.5}Rh_{0.5}$ presents a transition from an antiferromagnetic order to a ferromagnetic one at $T^* = 350$ K. Cherifi et al. showed that the application of an electric field to the BTO substrate induces a very large variation in the magnetization, arising from the E-field induced transformation from the AFM to the FM order. The E-field dependence of this variation, presented in Fig. 2H, mimics that of the strain, with an additional slight asymmetry that may be ascribed to polarization-charge effects.

The potential of this strain strategy for a low-power E-field control of a magnetization in heterostructures for spintronics such as spin valves or magnetic tunnel junctions (MTJs) used in non-volatile magnetic random access memories (MRAMs) has been also explored theoretically [49–51] and experimentally [52,53]. In spin valves or MTJs, the resistance depends on the relative orientation (either parallel or antiparallel) of the magnetizations of the two FM electrodes separated by either an ultrathin metallic (spin valves) or an insulating (MTJs) layer. This corresponds to the giant magnetoresistance (GMR) and to the tunnel magnetoresistance (TMR) in spin valves and MTJs, respectively. Using phase-field simulations, Hu et al. predicted an ultra-low writing energy (0.16 fJ/bit) together with a high storage density, a good thermal stability and a fast writing speed for E-field controlled MRAMs deposited on (011)-oriented PMN–PT [51].

Experimentally, Cavaco et al. demonstrated voltage-controlled changes in the resistance of an IrMn/$Co_{50}Fe_{50}$/Cu/$Co_{50}Fe_{50}$ spin valve [52]. The GMR curve they measured showed signs of exchange bias due to the presence of an IrMn film in contact with the hard magnetic CoFe layer. Upon application of an electric field, the coercivity of the $Co_{50}Fe_{50}$ free layer is changed, whereas the exchange bias is unaffected, as shown in Fig. 4A. Lei et al. evidenced similar changes in the GMR curves of a CoFeB/Cu/Co/IrMn spin valve deposited on PZT due to the large increase of the coercivity of the free layer under stress (Fig. 4B) [53]. Interestingly, Novosad et al. proposed a new concept of MRAM based on this strain strategy [54]. It is composed of an array of magnetostrictive ferromagnetic particles formed on a grid-patterned piezoelectric film in which a rotatable stress generated in the selected memory cell leads to the magnetization reversal of the particles.

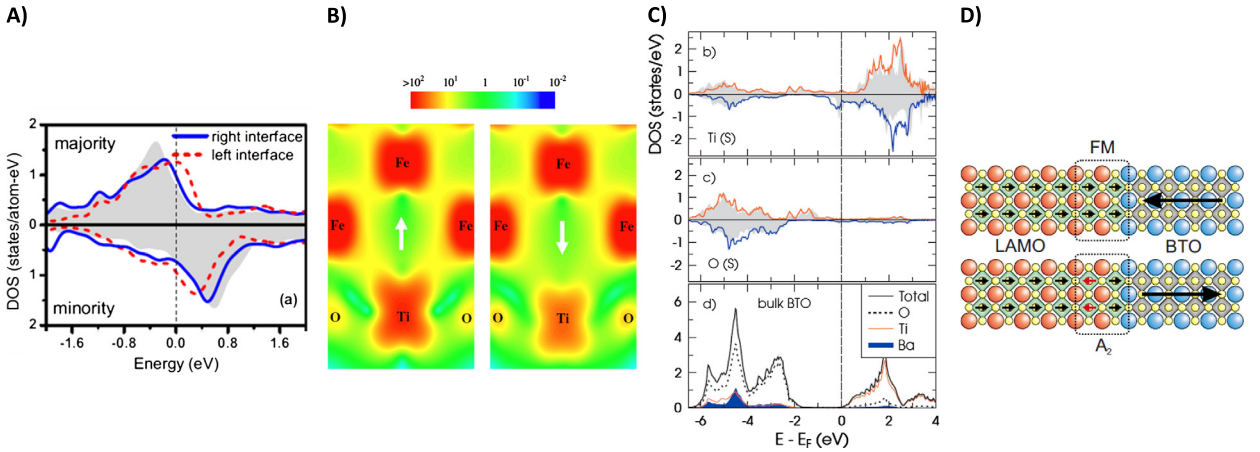

Fig. 5. (Color online.) A) Spin-polarized local density of states projected onto the Ru 3d orbitals for polarization pointing toward (right interface) or away from (left interface) the SRO layer in SRO/BTO(001) heterostructures. The shaded surface is the Ru 3*d* density of states in the bulk. Adapted from [58]. B) Minority-spin charge density (in arbitrary units) at the Fe/BTO interface for two opposite polarizations direction in BTO (indicated by the white arrow). The overlap between the Ti and Fe electronic clouds is much stronger when the FE polarization points toward Fe than in the opposite case, which reflects a stronger hybridization for the former. From [61]. C) Spin-resolved DOS of Ti (top) and O (middle) in the surface BTO layer at the interface with one monolayer of Fe for polarization pointing towards (lines) or away from (shaded gray surfaces) Fe, as well as the bulk DOS (bottom) of $BaTiO_3$. From [62] D) Electrically-induced magnetic reconstruction at the $La_{0.5}A_{0.5}MnO_3$/BTO interface (A = Ca, Sr, or Ba); The arrangement of the magnetic moments at Mn sites (small arrows) changes from FM to A-type antiferromagnetic as the FE polarization (large arrows) of the BTO is reversed. From [73].

However, strain-mediated ME coupling generally results in a less-than-90° rotation of the magnetization, whereas MRAMs are based on the 180° deterministic control of the magnetization. As such, strain-mediated ME coupling seems more promising for *E*-field tunable microwave magnetic devices.

2. Electronic effect in magnetoelectric multiferroics

Whereas a butterfly-shaped loop of magnetization vs. electric field mimicking that of strain vs. electric field, and revealing the elastic nature of the ME coupling, is observed in (La,Sr)MnO_3 (20 nm)/PMN–PT heterostructures (Fig. 2A) [13], a totally different square shape is obtained in (La,Sr)MnO_3 (4 nm)/PZT heterostructures (Fig. 6C) [55]. Indeed, for small thicknesses of the ferromagnetic film, interface-charge-mediated ME coupling was predicted to dominate the changes in the magnetic properties by polarization reversal [56]. For (La,Sr)MnO_3, a critical thickness of 4.2 nm was predicted to switch from strain-mediated to charge-mediated ME coupling.

The second type of ME coupling allowing an electric control of the magnetic properties in ferroelectric/magnetic bilayers is thus related to the influence of the FE polarization direction on the electronic structure of the ferromagnet at the interface. Interestingly, such electronic effects depend on the FE polarization direction and can produce two different magnetic states at electrical remanence. This electronically-driven ME coupling is thus not only interesting from a fundamental point of view, but is also highly promising for applications. However, while the elastic interaction can extend over several hundreds of nanometers, the field effect operates over distances of the order of the Thomas–Fermi screening length (λ_{TF}), which is one or two unit cells for metals and few nanometers for semiconductors. Fortunately, in magnetic materials, changes in the magnetic properties may be perceived over distances set by the exchange interaction length, l_{ex}, which is usually larger than λ_{TF} and can approach 10 nm [57].

Several mechanisms take place to electronically drive changes in the magnetic properties.

The first mechanism is related to the spin-dependent screening in the FM of the interface-bound charges of the FE. In FM metals, due to the different density of states for spin up and spin down electrons at the Fermi level, the screening is spin dependent. This spin-dependent screening leads to notable changes in the surface magnetization and surface magnetocrystalline anisotropy. Such changes were predicted for the $SrRuO_3$ (SRO)/BTO system [58], for example. Fig. 5A shows the modification in the spin-polarized density of states (DOS) of SRO depending on the direction of the BTO FE polarization (right (left) interface corresponds to a polarization pointing to (away from) SRO). The change in the magnetic moment related to polarization reversal is 0.31 μ_B corresponding to a surface magnetoelectric coefficient $\alpha = 2.3 \times 10^{-10}$ Oe·cm^2·V^{-1} [58]. Cai et al. proposed to exploit this mechanism to obtain large magnetoelectric effects in normal-metal/FE/FM-metal heterostructures due to the combination of broken inversion symmetry at both interfaces and spin-dependent screening in the FM [59]. Nevertheless, this large effect, larger than strain-mediated magnetoelectric coupling, is localized at the interface and superlattices have to be considered to obtain a sizable change in the measured magnetic moment [60].

The second contribution to the ME effect is due to a change in the electronic bonding at the interface between the FE and the FM. The displacements of atoms in the FE due to the polarization reversal alter the overlap between the orbital of the FE and FM compounds at the interface. This results in different charge transfers, which affects the interface magnetization, anisotropy, and spin polarization (see Fig. 5B). This interface-bonding-mechanism-ME effect has been predicted to play a

significant role for Fe/BTO or Fe/$PbTiO_3$ (PTO) [61–63], Co_2MnSi/BTO [64], Fe_3O_4/BTO [65], Co/BTO [66] and Co/PVDF [67]. A large ME coupling coefficient defined as $\alpha_s = \mu_0 \Delta M_s / E$ of the order of 10^{-2} Oe·cm·V^{-1} was found in the case of 1 monolayer (ML) Fe/BTO or Fe/PTO [61]. Theoretical studies on Fe/(BTO, PTO) systems also predicted a sizable magnetic moment on the Ti cation (Fig. 5C) [61,62]. This was confirmed recently by X-ray resonant magnetic scattering experiments [68,69]. This Ti moment is sensitive to ferroelectric displacement and should thus change depending on the direction of the FE polarization [61,62].

Large changes in magnetocrystalline anisotropy, of up to 50%, associated with the variation in the orbital occupancy upon polarization reversal were also reported in Fe/BTO [70] and FePt/BTO [71] systems.

Interestingly, similar modulations of the magnetic moment and magnetocrystalline anisotropy were predicted for Co/PVDF [67] and Fe/PVDF [72], with a possible switch from in-plane to out-of-plane magnetization easy axis.

Another magnetoelectric effect at the ferromagnet/ferroelectric interface is related to the magnetic reconstruction induced by the switching of the ferroelectric polarization. Although the driven force is also based on screening charges, the change in surface magnetization does not result from a variation in the magnitude of local magnetic moments, but instead from a change in how these magnetic moments are ordered near the interface. Such effect is particularly appealing in materials such as manganites possessing very rich phase diagrams, with competing magnetic phases, as a function of carrier doping. In this case, the change in the magnetic state results from the competition between superexchange interaction, which promotes antiparallel alignment of neighboring Mn magnetic moments, and the double-exchange interaction, which favors their parallel arrangement. This effect has been predicted using first-principles calculations for the $La_{1-x}A_xMnO_3/BaTiO_3$ (001) interface for a concentration ($x = 0.5$) close to the ferromagnetic–antiferromagnetic phase transition [73]. For this bilayer, a ferromagnetic configuration is stabilized at the interface when the polarization in BTO points toward the interface (depleted hole state), whereas an antiferromagnetic phase extending over two unit cells is stabilized when the FE polarization points away from the manganite (accumulated hole state) (Fig. 5D). As a result of this ferroelectrically-driven magnetic reconstruction, a very large magnetoelectric coefficient resulting from the large change in magnetic moment is deduced: $\alpha_s = 5.3 \cdot 10^{-9}$ Oe·cm^2·V^{-1} [73]. Magnetic phase transitions induced by polarization reversal were also predicted in FE-field effect transistors (FE-FET) with a magnetic electrode [74].

The electronically-driven ME coupling could thus induce changes in the saturation magnetization, the interface magnetocrystalline anisotropy, the magnetic state at the interface and its possible combinations. Interestingly, even if the change in the magnetization is small and localized at the interface and thus difficult to exploit, the modulation of the spin polarization can also be large. Since the interfacial spin-polarization controls the amplitude of the TMR, a clever way to exploit the modification in the DOS at the Fermi level depending on the ferroelectric polarization direction is to build ferromagnetic tunnel junctions, including a ferroelectric tunnel barrier [75].

Charge-driven magnetoelectric coupling is particularly efficient in ferromagnets in which the magnetism is carrier-mediated, such as diluted magnetic semiconductors (DMS) or manganites. Experimentally, following the first demonstration of an electric control of the magnetic state of the carrier mediated FM material (In,Mn)As by applying a gate voltage to an (In,Mn)As channel in a field effect transistor (FET) [76], a non-volatile E-field tuning of the magnetic configuration from a ferromagnetic state (accumulation) to a paramagnetic (depletion) one was demonstrated a few years later by replacing the dielectric gate by a FE one [77] (see Fig. 6A top). In this FE/DMS architecture, the control of the Curie temperature of the 7-nm (Ga,Mn)As channel over a few kelvins was also shown through a shift of the maximum in the resistance versus temperature curve induced by reversing the polarization direction of the polyvinylidene fluoride with trifluoroethylene (PVDF–TrFE) gate (see Fig. 6A, bottom). The mechanism at the origin of the effect is the polarization-induced depletion or accumulation of holes in the channel at the origin of the magnetic interaction in the channel.

Similar studies were performed on manganites, compounds in which the rich-phase diagram strongly depends on the carrier doping concentration [78]. This control can be anticipated from the changes observed in the metal–insulator transition temperature [79] or from the room-temperature modulation of the resistance [80] in manganite-based field effect transistors. For example, Kanki et al. [81] evidenced modifications in the magnetic moment amplitude of a 10-nm $La_{0.85}Ba_{0.15}MnO_3$ channel by XMCD experiments close to the metal–insulator transition temperature (see Fig. 6B, top panel). This modulation was associated with changes induced in the carrier concentration of the channel depending on the direction of the PZT ferroelectric gate polarization at remanence, as revealed by the resistance dependence presented in Fig. 6B (bottom panel). Lu et al. observed 10% modulations of the magnetization by polarization reversal in $La_{0.67}Sr_{0.33}MnO_3$ (10nm)/BTO bilayers grown on $SrTiO_3$(001) substrates [82]. The large change in magnetization, inversely proportional to the $La_{0.67}Sr_{0.33}MnO_3$ thickness, was attributed to both, the carrier modulation and the shift in the metal–insulator transition close to room temperature due to carrier doping. Interestingly, the third mechanism, i.e., an electrically induced magnetic transition, has been clearly identified to play a drastic role in $La_{0.8}Sr_{0.2}MnO_3$ (4-nm)/PZT bilayers [55]. Important modifications in both the Curie temperature (see Fig. 6C) and magnetization amplitude at 100 K probed by Kerr magnetometry (insert of Fig. 6C) were reported in this system. These changes correspond to a large magnetoelectric coupling of the order of 10^{-3} Oe·cm·V^{-1}. Additional experiments using X-ray absorption near-edge spectroscopy revealed the charge-induced change by polarization switching in the valence state of Mn atoms (0.1 electrons per Mn atom) in the $La_{0.8}Sr_{0.2}MnO_3$ layer [83]. From combined spectroscopic, magnetic, and electric characterizations of this system, Vaz et al. concluded that the magnetic spin configuration of the $La_{0.8}Sr_{0.2}MnO_3$ at the PZT interface changes from ferromagnetic in the depletion state to A-type antiferromagnetic in the accumulation state (increase of hole doping) and that this interface-charge-driven ME coupling is at the origin of the effect [84]. In the accumulation state, the interface layer consists of strongly depopulated, antibonding 3d $e_g 3z^2–r^2$ states,

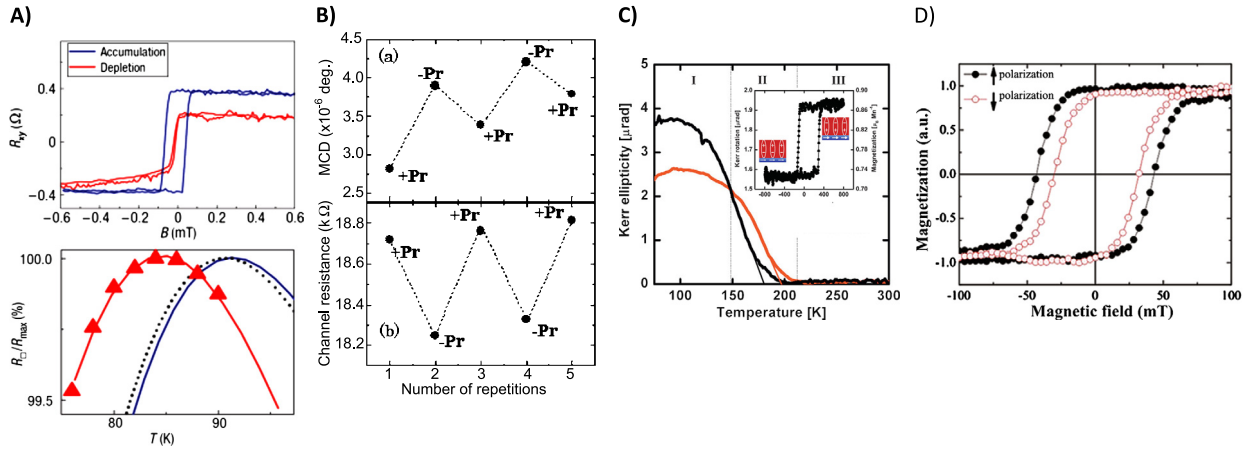

Fig. 6. (Color online.) A) Top: R_{Hall} vs. magnetic field at 60 K of a PVDF–TrFE/(Ga, Mn)As FE-FET. In the depletion state, the hysteresis cannot be resolved (paramagnetic state), whereas in the accumulation state, it is clearly observed in agreement with carrier-mediated ferromagnetism in DMS. Bottom: Resistance vs. temperature for a PVDF–TrFE/(Ga, Mn)As FE-FET. The maxima indicate the Curie temperature (T_C). In the depletion state, the T_C shifts toward lower temperatures. From Ref. [77]. B) Changes in the amplitude of the magnetic moment revealed by XMCD measurements (top) and electrical properties (bottom) at FE remanence due to repetitive switching of the ferroelectric polarization in PZT/$La_{0.85}Ba_{0.15}MnO_3$ heterostructures. From [81]. C) Temperature dependence of the magnetization of a 4-nm $La_{0.8}Sr_{0.2}MnO_3$ film on PZT. A 20-K variation of T_C is observed between the two FE polarization states. Inset: Magnetoelectric hysteresis at 100 K during ferroelectric polarization reversal. From [55]. D) Out of plane hysteresis loops of a 0.95 nm Co layer deposited on 30 unit cells of PVDF–TrFE after switching the FE polarization up (black curve) or down (red one). From [86].

resulting in a weakening of the double-exchange interaction at these orbitals. An antiferromagnetic coupling to the adjacent layers ensures that the 3d $e_g x^2-y^2$ orbitals are energetically privileged, favoring the superexchange interaction and a transition from a ferromagnetic state to an antiferromagnetic one, in agreement with theoretical predictions for similar systems [73]. More recently, Ma et al. [85] revealed a large change (by one order of magnitude) in the in-plane and out-of-plane magnetizations at the $La_{0.67}Sr_{0.33}MnO_3$/PZT interface related to the appearance of an antiferromagnetic spin alignment by hole doping. They used magnetic second-harmonic generation, a technique sensitive to the interface, at 78 K.

To obtain an electric control at room temperature, transition metals and alloys have to be considered instead of strongly correlated materials. Experiments showing the electrical control of magnetic anisotropy via electronic effects on transition metals are scarce and a full FE control of the magnetization easy axis has not been provided. Nevertheless, a substantial variation of the coercive field, reflecting changes in the magnetic anisotropy, was reported in ultrathin Co films combined with a PVDF–TrFE ferroelectric gate. The hysteretic behavior, observed in the coercive field versus the electric field (Fig. 6D), mimics that of the polarization [86]. Changes in the magnetization by polarization reversal in the Fe/BTO model system has not been demonstrated experimentally, but the predicted variations of the magnetic moment are small, 0.1 μ_B/Fe and localized at the interface [61,62]. Nevertheless, the related modulation of the spin polarization at the interface has been successfully evidenced in $La_{0.67}Sr_{0.33}MnO_3$/BTO/Fe multiferroic tunnel junctions [75]. In these junctions, the electric modulation of the transport properties arises from two effects [87–89]. The first one is the modulation of the tunnel barrier height by the polarization reversal [90,91], giving rise to large tunnel electroresistance phenomena [92–97]. This large modulation of the tunneling current together with the large readout current densities are appealing skills of these ferroelectric tunnel junctions to design a new generation of non-volatile FE memories with non-destructive readout [92]. Furthermore, the multistate resistance correlated with the FE domain configuration is another appealing attribute of these junctions that can be considered as a new kind of memristor [98,99] that could act as artificial synapses in neuromorphic architectures. The second one is the electrically controlled change in the spin polarization at the interface that sets the amplitude of the tunnel TMR. Garcia et al. (Fig. 7A) showed that in these multiferroic tunnel junctions, the reversal of the ferroelectric polarization in the barrier induces a sizable modification in the amplitude of the TMR effect by 450%, reflecting the FE non-volatile modulation of the spin polarization of Fe at the interface with $BaTiO_3$ [75]. Similar results were obtained in $La_{0.67}Sr_{0.33}MnO_3$/BTO/Co [69] and $La_{0.67}Sr_{0.33}MnO_3$/PZT/Co systems [100]. In the latter case, Pantel et al. reported an inversion in the sign of the TMR—associated with the sign inversion of the spin polarization of Co—induced by polarization switching (see Fig. 7B). Because these tunnel junctions contain a half-metallic $La_{0.67}Sr_{0.33}MnO_3$ bottom electrode that loses its spin polarization just below 300 K [101], these results were obtained at low temperatures. These multiferroic tunnel junctions thus allow one to obtain four resistance states and provide an interesting alternative way to control spin polarization, i.e. no more with a magnetic field, but with an electric one.

3. Other mechanisms based on intrinsic multiferroics

Another way to electrically control magnetization is offered in heterostructures combining a multiferroic or magnetoelectric material and a FM coupled by exchange-bias interaction. Most multiferroic materials are ferroelectric antiferromagnets (AFMs). The ME coupling in these materials thus links the AFM and FE orders and allows an electric control of the AFM

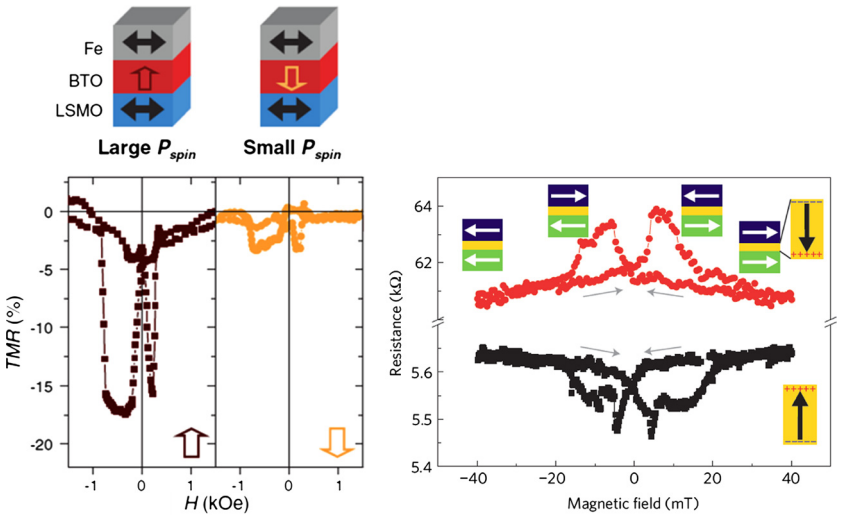

Fig. 7. (Color online.) A) Resistance vs. magnetic field (TMR) of a $La_{0.67}Sr_{0.33}MnO_3$/BTO/Fe tunnel junction measured at electrical remanence and 4 K, after switching the FE polarization up or down. The large variation of the TMR reflects changes in the interfacial Fe spin polarization due to FE polarization reversal. From [75]. B) Resistance vs. magnetic field at 50 K in the as-grown state of a $La_{0.67}Sr_{0.33}MnO_3$/PZT/Co junction (black squares) and after polarization switching (red circles). From [100]. The FE polarization states of the barrier as well as the magnetization directions in the electrodes are shown by arrows.

spin configuration. Cooling FM/AFM heterostructures in the presence of a magnetic field across the Néel temperature of the AFM induces a shift of the hysteresis loop of the FM [102]. The magnitude of this shift is the exchange-bias field, which is generally in the opposite direction to the cooling field. The mechanism for this exchange-bias interaction is still subject to debate, but is generally attributed to uncompensated spins at the interface between the AFM and the FM. Interestingly, the E-field control of the exchange bias could result in a 180° magnetization direction change of the FM and enables novel concepts of electrically-controlled magnetic memories [103–105]. The first demonstration of an electric control of the exchange-bias interaction was reported using the magnetoelectric Cr_2O_3 [106]. Cr_2O_3 is an AFM magnetoelectric material with a Néel temperature $T_N = 307$ K. Below T_N, the application of an electric field across Cr_2O_3 induces a net magnetization, whose direction depends on the sign of the electric field. This net magnetization can be used to electrically manipulate the magnetization of an exchange-coupled FM film [107]. This was first demonstrated for a Pt/Co bilayer deposited on a Cr_2O_3 (111) crystal. Either a positive or negative shift of the hysteresis was observed after complicated cooling processes across T_N that implicated both electric and magnetic fields [106]. Each sign reversal of the exchange-bias field required new magnetoelectric annealing. Reversible and isothermal control of the exchange bias using Cr_2O_3 was later demonstrated for a Co/Pd/Cr_2O_3 heterostructure at constant magnetic field using the sign of the electric field to control the AFM domain state and switch the exchange-bias field [108].

More promising for application is the electric control of exchange bias directly using an antiferromagnetic–FE multiferroic since it allows one to control magnetization at electrical remanence. This route was explored for $YMnO_3$/NiFe bilayers by Laukhin et al. [109]. In bulk, hexagonal $YMnO_3$ is a robust ferroelectric (with a T_C of 900 K) that presents an AFM behavior below 90 K with coupled order parameters at DWs [110]. Fig. 8A shows magnetization loops under various biasing voltages, at 2 K after cooling the sample from 300 K under an applied field of 3 kOe. The clear shift of the loops reflects the existence of a large exchange-bias field that gradually disappears upon application of the biasing voltage and cancels out at 1.2 V. This suppression was confirmed by the transition from a $\sin\theta$ to a $\sin^2\theta$ dependence of the anisotropic magnetoresistance when the voltage was applied. Unfortunately these changes were not reversible. Later on, the same group extended the investigations toward the non-ferroelastic FE-AFM $LuMnO_3$ and reported the E-field control of the magnetization of a coupled NiFe film at 5 K [111]. Under the application of a magnetic and of an electric field of suitable amplitude and duration, the exchange bias could be restored, making the effect reversible. The observed effect was independent of the polarity of the applied voltage, but depended on the duration of the pulse. These results were interpreted in terms of the electric-field-pulse-induced declamping of coupled AFM–DWs/FE–DWs [110] in this multiferroic material, and the resulting change in the exchange bias related to the coupling of the magnetic moment of NiFe with pinned uncompensated moments at the AFM–DW.

To obtain such control at room temperature, several groups explored the potential of $BiFeO_3$ (BFO), one of the only multiferroic material at room temperature with a robust antiferromagnetic ($T_N = 643$ K) and FE ($T_C = 1100$ K) orders and a very large polarization along the [111] direction (100 μC/cm^2) [112]. Whereas in bulk the net magnetic moment resulting from a Dzyaloshinskii–Moriya interaction is averaged to zero by an additional cycloidal modulation [113], it is non-zero in thin films [114,115]. In BFO thin films, a strong internal magnetoelectric coupling locally links the net moment to the direction of the FE polarization and allows a switching of the AFM domains when the FE polarization in BFO rotates by 109° or 71° [116]. BFO is thus a promising material to obtain a room-temperature electrically controllable exchange-biased

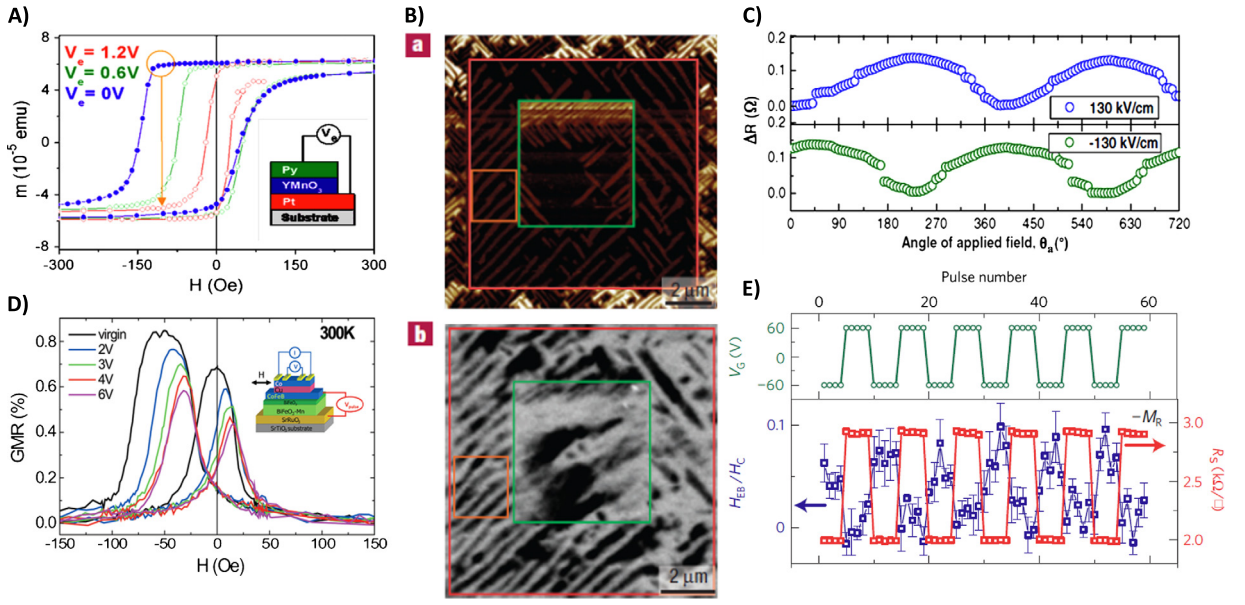

Fig. 8. (Color online.) A) Magnetization loops of NiFe/$YMnO_3$/Pt heterostructures, measured at 2 K, after cooling the sample from 300 K in a 3-kOe field, under various biasing-voltage (V_e) values. Adapted from Ref. [109]. B) Microscopic evidence for magnetoelectric coupling: a) in-plane PFM image showing the FE domain pattern of a BFO thin film; b) corresponding FM domain pattern of a $Co_{0.9}Fe_{0.1}$ film grown on BFO revealed by XMCD-PEEM. From [120]. C) Anisotropic magnetoresistance of a $Co_{0.9}Fe_{0.1}$ layer coupled to BFO after applying a $\pm$ 130 kV/cm electric field across the FE. The 180° shift of the signal indicates the reversal of the $Co_{0.9}Fe_{0.1}$ magnetic moment [121]. D) GMR curves of an Au 6-nm/Co 4-nm/Cu 4-nm/$Co_{0.72}Fe_{0.08}B_{0.20}$ 4-nm spin valve deposited onto a BFO/BFO:Mn bilayer after applying different E-fields across the FE. Adapted from [117]. E) Electric control of the exchange bias at 5.5 K in a field effect device with a $La_{0.7}Sr_{0.3}MnO_3$ channel and a gate of BFO. The normalized exchange bias was determined from magnetoresistance measurements after pulsing the gate with voltage V_G. From [127].

system when coupled with FMs possessing large Curie temperatures, such as transition metals Fe, Co, Ni [117], or alloys such as NiFe [118,119], FeCo [120,121], or CoFeB [122]. Two distinct types of interactions, i.e. a large shift of the hysteresis loop (exchange bias) or/and an enhancement of the coercive field, have been observed in these heterostructures depending on the morphology of the films [123]. Whereas for stripe-like ferroelectric domains in BFO, only an increase of the coercive field is observed, in mosaic-like domains a clear shift of the hysteresis loop is observed, revealing a large exchange bias. This exchange bias arises from the coupling between the magnetization of the FM layer and uncompensated spins at FE-AFM DWs [124], more precisely at 109° DWs [123,125]. Using stripe-like domains, Chu et al. [120], and more recently Heron et al. [121] combined PFM and XMCD-PEEM to provide direct evidence of the nearly perfect matching between the FE domains of BFO and the FM ones in a top $Co_{0.9}Fe_{0.1}$ thin film with submicrometer resolution (see Fig. 8B). They also evidenced that in a planar geometry, the direction of the magnetization of the $Co_{0.9}Fe_{0.1}$ could be switched electrically and reversibly at room temperature by modifying the FE domain structures of BFO. This was evidenced from the anisotropic magnetoresistance measurements presented in Fig. 8C [121] with a voltage induced inversion of the sin θ dependence, reflecting a macroscopic switch of the net magnetization direction by 180°.

Exploiting the large exchange bias existing in mosaic-like BFO/FM, Allibe et al. optimized the exchange bias, the ferroelectric properties and the GMR of CoFeB/Cu/Co spin valves on BFO/BFO:Mn bilayers [126] and demonstrated the control of the GMR response upon the application of a modest voltage across the multiferroic resulting in a strong reduction of the exchange bias at room temperature (Fig. 8D) [117]. However, the effect proved to be irreversible.

Reversible electric control of the exchange bias was also reported in BFO/$La_{0.7}Sr_{0.3}MnO_3$ field-effect heterostructures. As shown in Fig. 8E, the sign of the exchange bias at 5.5 K can be reproducibly modified by switching the ferroelectric polarization of BFO [127]. As it was independent of the ferroelectric DW type and density, the exchange bias in this system has been linked to the formation of a ferromagnetic moment in BFO that is coupled to the magnetism of the adjacent $La_{0.7}Sr_{0.3}MnO_3$ layer [128]. This induced magnetic moment was predicted to result from the competition between ferromagnetic double-exchange and antiferromagnetic super-exchange interactions. The balance between these ferromagnetic and antiferromagnetic tendencies is strongly affected by the interfacial electronic charge density that can be controlled by the direction of the BFO FE polarization [129].

4. Concluding remarks

In this review, we summarized the progress in the field of artificial multiferroic heterostructures combining ferroelectric and ferromagnetic materials, which expanded tremendously during the past ten years. Very large magnetoelectric couplings, much larger than those of intrinsic multiferroics, were measured due to either strain-mediated or electronic effects at inter-

faces or a combination of thereof. This large ME coupling has been successfully exploited to obtain an electric control of the magnetization amplitude, anisotropy, spin polarization, or Curie temperature. To obtain an electrically-induced 180° rotation of the magnetization of interest for spintronics, the electronic strategy seems more promising, even if not yet demonstrated. Another strategy developed to obtain an electric control of magnetization was to exploit the exchange bias at the interface between antiferromagnetic–ferroelectric intrinsic multiferroics and ferromagnets. This latter strategy seems promising, since pure electric switching of the magnetization of a transition metal alloy has been demonstrated in a planar geometry. Future work in a vertical one should allow us to obtain the desired electric control of a spin valve compatible with MRAMs design. On route towards this goal, several other interesting phenomena appeared such as the opportunity to electrically tune the spin polarization of a ferromagnet that can be exploited in magnetic tunnel junctions with a ferroelectric tunnel barrier. Another is the demonstration of the electrical control of a magnetic phase transition. Additionally, the field of research concerning the electrical control of a perpendicular magnetization based upon the Rashba spin–orbit interaction in asymmetric heterostructure is of great promise and rapidly expanding.

Acknowledgements

This work received financial support from the European Research Council Advanced Grant FEMMES (contract No. 267579).

References

[1] H. Schmidt, Multi-ferroic magnetoelectrics, Ferroelectrics 162 (1994) 317–338.
[2] M. Fiebig, Revival of the magnetoelectric effect, J. Phys. D, Appl. Phys. 38 (2005) R123–R152.
[3] W. Eerenstein, N.D. Mathur, J.F. Scott, Multiferroic and magnetoelectric materials, Nature 442 (2006) 759–765.
[4] N.A. Hill, Why are there so few magnetic ferroelectrics?, J. Phys. Chem. B 104 (2000) 6694–6709.
[5] C.W. Nan, M.I. Bichurin, S.X. Dong, D. Viehland, G. Srinivasan, Multiferroic magnetoelectric composites: historical perspective, status, and future directions, J. Appl. Phys. 103 (2008) 031101.
[6] C.A.F. Vaz, J. Hoffman, C.H. Ahn, R. Ramesh, Magnetoelectric coupling effects in multiferroic complex oxide composite structures, Adv. Mater. 22 (2010) 2900–2918.
[7] J. Ma, J.-M. Hu, Z. Li, C.-W. Nan, Recent progress in multiferroic magnetoelectric composites: from bulk to thin films, Adv. Mater. 23 (2011) 1062–1087.
[8] R.C. Kambale, D.Y. Jeong, J. Ryu, Current status of magnetoelectric composite thin/thick films, Adv. Condens. Matter Phys. 2012 (2012) 824643.
[9] C.A.F. Vaz, Electric field control of magnetism in multiferroic heterostructures, J. Phys. Condens. Matter 24 (2012) 333201.
[10] S. Fusil, V. Garcia, A. Barthélémy, M. Bibes, Magnetoelectric devices for spintronics, Annu. Rev. Mater. Res. 44 (2014) 91–116.
[11] Y. Wang, J.M. Hu, Y.H. Lin, C.-W. Nan, Multiferroic magnetoelectric composite nanostructures, NPG Asia Mater. 2 (2010) 61–68.
[12] C.W. Nan, Magnetoelectric effect in composites of piezoelectric and piezomagnetic phases, Phys. Rev. B 50 (1994) 6082–6088.
[13] C. Thiele, K. Dorr, O. Bilani, J. Rödel, L. Schultz, Influence of strain on the magnetization and magnetoelectric effect in $La_{0.7}A_{0.3}MnO_3$/PMN–PT(001) (A = Sr, Ca), Phys. Rev. B 75 (2007) 054408.
[14] G. Venkataiah, Y. Shirahata, M. Itoh, T. Taniyama, Manipulation of magnetic coercivity of Fe film in Fe/$BaTiO_3$ heterostructure by electric field, Appl. Phys. Lett. 99 (2011) 102506.
[15] Y. Shirahata, T. Nozaki, G. Venkataiah, H. Taniguchi, M. Itoh, T. Taniyama, Switching of the symmetry of magnetic anisotropy in Fe/$BaTiO_3$ heterostructures, Appl. Phys. Lett. 99 (2011) 022501.
[16] N.A. Pertsev, Giant magnetoelectric effect via strain-induced spin reorientation transitions in ferromagnetic films, Phys. Rev. B 78 (2008) 212102.
[17] J.-M. Hu, C.-W. Nan, Electric-field-induced magnetic easy-axis reorientation in ferromagnetic/ferroelectric layered heterostructures, Phys. Rev. B 80 (2009) 224416.
[18] M.K. Lee, T.K. Nath, C.B. Eom, M.C. Smoak, F. Tsui, Strain modification of epitaxial perovskite oxide thin films using structural transitions of ferroelectric $BaTiO_3$ substrate, Appl. Phys. Lett. 77 (2000) 3547–3549.
[19] W. Eerenstein, M. Wiora, J.L. Prieto, J.F. Scott, N.D. Mathur, Giant sharp and persistent converse magnetoelectric effects in multiferroic epitaxial heterostructures, Nat. Mater. 6 (2007) 348–351.
[20] C.A.F. Vaz, J. Hoffman, A.B. Posadas, C. Ahn, Magnetic anisotropy modulation of magnetite in Fe_3O_4/$BaTiO_3$(100) epitaxial structures, Appl. Phys. Lett. 94 (2009) 022504.
[21] R.V. Chopdekar, Y. Suzuki, Magnetoelectric coupling in epitaxial $CoFe_2O_4$ on $BaTiO_3$, Appl. Phys. Lett. 89 (2006) 182506.
[22] T.H.E. Lahtinen, S. van Dijken, Temperature control of local magnetic anisotropy in multiferroic CoFe/$BaTiO_3$, Appl. Phys. Lett. 102 (2013) 112406.
[23] R. Moubah, F. Magnus, A. Zamani, V. Kapaklis, P. Nordblad, B. Hjörvarsson, Strain induced changes in magnetization of amorphous $Co_{95}Zr_5$ based multiferroic heterostructures, AIP Adv. 3 (2013) 022113.
[24] S. Polisetty, W. Echtenkamp, K. Jones, X. He, S. Sahoo, C. Binek, Piezoelectric tuning of exchange bias in a heterostructure, Phys. Rev. B 82 (2010) 134419.
[25] K. Dörr, C. Thiele, Multiferroic bilayers of manganites and titanates, Phys. Stat. Sol. (b) 243 (2006) 21–28.
[26] T. Nan, Z. Zhou, M. Liu, X. Yang, Y. Gao, B.A. Assaf, H. Lin, S. Velu, X. Wang, H. Luo, J. Chen, S. Akhtar, E. Hu, R. Rajiv, K. Krishnan, S. Sreedhar, D. Heiman, B.M. Howe, G.J. Brown, N.X. Sun, Quantification of strain and charge co-mediated magnetoelectric coupling on ultra-thin Permalloy/PMN–PT interface, Sci. Rep. 4 (2014) 03688.
[27] S. Geprags, A. Brandlmaier, M. Opel, et al., Electric field controlled manipulation of the magnetization in Ni/$BaTiO_3$ hybrid structures, Appl. Phys. Lett. 96 (2010) 142509.
[28] M. Weiler, A. Brandlmaier, S. Geprags, N. Althammer, M. Opel, C. Bihler, H. Huebl, M.S. Brandt, R. Gross, S.T. Goennenwein, Voltage controlled inversion of magnetic anisotropy in a ferromagnetic thin film at room temperature, New J. Phys. 11 (2009) 013021.
[29] A. Brandlmaier, S. Geprägs, G. Woltersdorf, R. Gross, S.T.B. Goennenwein, Nonvolatile, reversible electric-field controlled switching of remanent magnetization in multifunctional ferromagnetic/ferroelectric hybrids, J. Appl. Phys. 110 (2011) 043913.
[30] Ming Liu, Jing Lou, Shandong Li, Nian X. Sun, *E*-field control of exchange bias and deterministic magnetization switching in AFM/FM/FE multiferroic heterostructures, Adv. Funct. Mater. 21 (2011) 2593–2598.
[31] T. Wu, A. Bur, P. Zhao, K.P. Mohanchandra, K. Wong, K.L. Wang, C.S. Lynch, G.P. Carman, Giant electric-field-induced reversible and permanent magnetization reorientation on magnetoelectric Ni/(011)[$Pb(Mg_{1/3}Nb_{2/3})O_3$](1 − *x*)–[$PbTiO_3$]$_x$ heterostructure, Appl. Phys. Lett. 98 (2011) 012504.
[32] J. Lou, M. Liu, D. Ree, N.X. Sun, Giant electric field tuning of magnetism in novel multiferroic FeGaB/lead zinc niobate-lead titanate (PZN–PT) heterostructures, Adv. Mater. 21 (2009) 4711–4715.

[33] M. Liu, O. Obi, J. Lo, Y. Chen, Z. Cai, S. Stoute, M. Espanol, M. Lew, X. Situ, K.S. Ziemer, V.G. Harris, N.X. Sun, Giant electric field tuning of magnetic properties in multiferroic ferrite/ferroelectric heterostructures, Adv. Funct. Mater. 19 (2009) 1826–1831.
[34] M. Liu, S. Li, Z. Zhou, S. Beguhn, J. Lou, F. Xu, T.J. Lu, N.X. Sun, Electrically induced enormous magnetic anisotropy in Terfenol-D/lead zinc niobate-lead titanate multiferroic heterostructures, J. Appl. Phys. 112 (2012) 063917.
[35] T.K. Chung, G.P. Carman, K.P. Mohanchandra, Reversible magnetic domain-wall motion under an electric field in a magnetoelectric thin film, Appl. Phys. Lett. 92 (2008) 112509.
[36] T.H.E. Lahtinen, J.O. Tuomi, S. van Dijken, Pattern transfer and electric-field-induced magnetic domain formation in multiferroic heterostructures, Adv. Mater. 23 (2011) 3187–3191.
[37] T.H.E. Lahtinen, K.J.A. Franke, S. van Dijken, Electric-field control of magnetic domain wall motion and local magnetization reversal, Sci. Rep. 2 (2012) 258.
[38] R.V. Chopdekar, V.K. Malik, A. Fraile Rodríguez, L. Le Guyader, Y. Takamura, A. Scholl, D. Stender, C.W. Schneider, C. Bernhard, F. Nolting, L.J. Heyderman, Spatially resolved strain-imprinted magnetic states in an artificial multiferroic, Phys. Rev. B 86 (2012) 014408.
[39] B. Van de Wiele, L. Laurson, K.J.A. Franke, S. van Dijken, Electric field driven magnetic domain wall motion in ferromagnetic–ferroelectric heterostructures, Appl. Phys. Lett. 104 (2014) 012401.
[40] S.S.P. Parkin, M. Hayashi, L. Thomas, Magnetic domain-wall racetrack memory, Science 320 (2008) 190–194.
[41] D.A. Allwood, G. Xiong, C.C. Faulkner, D. Atkinson, D. Petit, R.P. Cowburn, Magnetic domain-wall logic, Science 309 (2005) 1688–1692.
[42] R.K. Zheng, Y. Wang, H.L.W. Chan, C.L. Choy, H.S. Luo, Strain-mediated electric-field control of resistance in the $La_{0.85}Sr_{0.15}MnO_3$/$0.7Pb(Mg_{1/3}Nb_{2/3})O_3$–$0.3PbTiO_3$ structure, Appl. Phys. Lett. 90 (2007) 152904.
[43] R.K. Zheng, Y. Wang, Y.K. Liu, G.Y. Gao, L.F. Fei, Y. Jiang, H.L.W. Chan, X.M. Li, H.S. Luo, X.G. Li, Epitaxial growth and interface strain coupling effects in manganite film/piezoelectric-crystal multiferroic heterostructures, Mater. Chem. Phys. 133 (2012) 42–46.
[44] Y.J. Yang, Z.L. Luo, M.M. Yang, H.L. Huang, H.B. Wang, J. Bao, G.Q. Pan, C. Gao, Q. Hao, S.T. Wang, M. Jokubaitis, W.Z. Zhang, G. Xiao, Y.P. Yao, Y.K. Liu, X.G. Li, Piezo-strain induced non-volatile resistance states in (011)–$La_{2/3}Sr_{1/3}MnO_3$/$0.7Pb(Mg_{2/3}Nb_{1/3})O_3$–$0.3PbTiO_3$ epitaxial heterostructures, Appl. Phys. Lett. 102 (2013) 033501.
[45] Z.G. Sheng, J. Gao, Y.P. Sun, Coaction of electric field induced strain and polarization effects in $La_{0.7}Ca_{0.3}MnO_3$/PMN–PT structures, Phys. Rev. B 79 (2009) 174437.
[46] R.K. Zheng, Y. Wang, H.L.W. Chan, C.L. Choy, H.S. Luo, Substrate-induced strain effect in $La_{0.875}Ba_{0.125}MnO_3$ thin films grown on ferroelectric single-crystal substrates, Appl. Phys. Lett. 92 (2008) 082908.
[47] Q.P. Chen, J.J. Yang, Y.G. Zhao, S. Zhang, J.W. Wang, M.H. Zhu, Y. Yu, X.Z. Zhang, Z. Wang, B. Yang, D. Xie, T.L. Ren, Electric-field control of phase separation and memory effect in $Pr_{0.6}Ca_{0.4}MnO_3$/$Pb(Mg_{1/3}Nb_{2/3})_{0.7}Ti_{0.3}O_3$ heterostructures, Appl. Phys. Lett. 98 (2011) 172507.
[48] R.O. Cherifi, V. Ivanovskaya, L.C. Phillips, A. Zobelli, I.C. Infante, E. Jacquet, V. Garcia, S. Fusil, P.R. Briddon, N. Guiblin, A. Mougin, A.A. Ünal, F. Kronast, S. Valencia, B. Dkhil, A. Barthélémy, M. Bibes, Electric-field control of magnetic order above room temperature, Nat. Mater. 13 (2014) 345–351.
[49] N.A. Pertsev, H. Kohlstedt, Magnetic tunnel junction on a ferroelectric substrate, Appl. Phys. Lett. 95 (2009) 163503.
[50] N.A. Pertsev, H. Kohlstedt, Resistive switching via the converse magnetoelectric effect in ferromagnetic multilayers on ferroelectric substrates, Nanotechnology 21 (2010) 475202.
[51] J.-M. Hu, Z. Li, L.-Q. Chen, C.-W. Nan, High-density magnetoresistive random access memory operating at ultralow voltage at room temperature, Nat. Commun. 2 (2011) 553.
[52] C. Cavaco, M. van Kampen, L. Lagae, C. Borghs, A room-temperature electrical field-controlled magnetic memory cell, J. Mater. Res. 22 (2007) 2111–2115.
[53] N. Lei, T. Devolder, G. Agnus, P. Aubert, L. Daniel, J.-V. Kim, W. Zhao, T. Trypiniotis, R.P. Cowburn, C. Chappert, D. Ravelosona, P. Lecoeur, Strain-controlled magnetic domain wall propagation in hybrid piezoelectric/ferromagnetic structures, Nat. Commun. 4 (2013) 1378.
[54] V. Novosad, Y. Otani, A. Ohsawa, S.G. Kim, K. Fukamichi, J. Koike, K. Maruyama, O. Kitakami, Y. Shimada, Novel magnetostrictive memory device, J. Appl. Phys. 87 (2000) 6400–6402.
[55] H. Molegraaf, J. Hoffman, C. Vaz, et al., Magnetoelectric effects in complex oxides with competing ground states, Adv. Mater. 21 (2009) 3470.
[56] J.-M. Hu, C.-W. Nan, L.-Q. Chen, Size-dependent electric voltage controlled magnetic anisotropy in multiferroic heterostructures: interface-charge and strain co-mediated magnetoelectric coupling, Phys. Rev. B 83 (2011) 134408.
[57] I.V. Ovchinnikov, K.L. Wang, Theory of electric-field-controlled surface ferromagnetic transition in metals, Phys. Rev. B 79 (2009) 020402(R).
[58] M.K. Niranjan, J.D. Burton, J.P. Velev, S.S. Jaswal, E.Y. Tsymbal, Magnetoelectric effect at the $SrRuO_3$/$BaTiO_3$ (001) interface: an ab initio study, Appl. Phys. Lett. 95 (2009) 052501.
[59] T. Cai, S. Ju, J. Lee, N. Sai, A.A. Demkov, Q. Niu, Z. Li, J. Shi, E. Wang, Magnetoelectric coupling and electric control of magnetization in ferromagnet/ferroelectric/normal-metal superlattices, Phys. Rev. B 80 (2009) 140415(R).
[60] J. Lee, N. Sai, T. Cai, Q. Niu, A.A. Demkov, Interfacial magnetoelectric coupling in tricomponent superlattices, Phys. Rev. B 81 (2010) 144425.
[61] C.G. Duan, S.S. Jaswal, E.Y. Tsymbal, Predicted magnetoelectric effect in Fe/$BaTiO_3$ multilayers: ferroelectric control of magnetism, Phys. Rev. Lett. 97 (2006) 047201.
[62] M. Fechner, I.V. Maznichenko, S. Ostanin, A. Ernst, J. Henk, P. Bruno, I. Mertig, Magnetic phase transition in two-phase multiferroics predicted from first principles, Phys. Rev. B 78 (2008) 212406.
[63] P.V. Lukashev, J.D. Burton, S.S. Jaswal, E.Y. Tsymbal, Ferroelectric control of the magnetocrystalline anisotropy of the Fe/$BaTiO_3$(001) interface, J. Phys. Condens. Matter 24 (2012) 226003.
[64] K. Yamauchi, B. Sanyal, S. Picozzi, Interface effects at a half-metal/ferroelectric junction, Appl. Phys. Lett. 91 (2007) 062506.
[65] M.K. Niranjan, J.P. Velev, C.-G. Duan, S.S. Jaswal, E.Y. Tsymbal, Magnetoelectric effect at the Fe_3O_4/$BaTiO_3$(001) interface: a first-principles study, Phys. Rev. B 78 (2008) 104405.
[66] D. Cao, M.-Q. Cai, W. Hu, C.-M. Xu, Magnetoelectric effect and critical thickness for ferroelectricity in Co/$BaTiO_3$/Co multiferroic tunnel junctions, J. Appl. Phys. 109 (2011) 114107.
[67] P.V. Lukashev, T.R. Paudel, J.M. Lopez-Encarnación, S. Adenwalla, E.Y. Tsymbal, J.P. Velev, Ferroelectric control of magnetocrystalline anisotropy at cobalt/poly(vinylidene fluoride) interfaces, ACS Nano 6 (2012) 9745–9750.
[68] S. Valencia, A. Crassous, L. Bocher, V. Garcia, X. Moya X, R.O. Cherifi, C. Deranlot, K. Bouzehouane, S. Fusil, A. Zobelli, A. Gloter, N.D. Mathur, A. Gaupp, R. Abrudan, F. Radu, A. Barthélémy, M. Bibes, Interface-induced room-temperature multiferroicity in $BaTiO_3$, Nat. Mater. 10 (2011) 753–758.
[69] L. Bocher, A. Gloter, A. Crassous, V. Garcia, K. March, A. Zobelli, S. Valencia, S. Enouz-Vedrenne, X. Moya, N.D. Mathur, C. Deranlot, S. Fusil, K. Bouzehouane, M. Bibes, A. Barthélémy, C. Colliex, O. Stephan, Atomic, electronic structure of the $BaTiO_3$/Fe interface in multiferroic tunnel junctions, Nano Lett. 12 (2012) 376–382.
[70] P.V. Lukashev, J.D. Burton, S.S. Jaswal, E.Y. Tsymbal, Ferroelectric control of the magnetocrystalline anisotropy of the Fe/$BaTiO_3$(001) interface, J. Phys. Condens. Matter 24 (2012) 226003.
[71] M. Lee, H. Choi, Y.-C. Chung, Ferroelectric control of magnetic anisotropy of FePt/$BaTiO_3$ magnetoelectric heterojunction: a density functional theory study, J. Appl. Phys. 113 (2013) 17C729.
[72] R.-Q. Wang, W.-J. Zhu, H.-C. Ding, S.-J. Gong, C.-G. Duan, Ferroelectric control of in-plane to out-of-plane magnetization switching at poly(vinylidene fluoride)/iron interface, J. Appl. Phys. 115 (2014) 043909.

[73] J.D. Burton, E.Y. Tsymbal, Prediction of electrically induced magnetic reconstruction at the manganite/ferroelectric interface, Phys. Rev. B 80 (2009) 174406.
[74] S. Dong, X. Zhang, R. Yu, J.-M. Liu, E. Dagotto, Microscopic model for the ferroelectric field effect in oxide heterostructures, Phys. Rev. B 84 (2011) 155117.
[75] V. Garcia, M. Bibes, L. Bocher, S. Valencia, F. Kronast, A. Crassous, X. Moya, S. Enouz-Vedrenne, A. Gloter, D. Imhoff, C. Deranlot, N.D. Mathur, K. Bouzehouane, A. Barthélémy, Ferroelectric control of spin polarization, Science 327 (2010) 1106–1110.
[76] H. Ohno, D. Chiba, F. Matsukura, T. Omiya, E. Abe, T. Dietl, Y. Ohno, K. Ohtani, Electric-field control of ferromagnetism, Nature 408 (2000) 944–946.
[77] I. Stolichnov, S.W.E. Riester, H.J. Trodah, N. Setter, A.W. Rushforth, K.W. Edmonds, R.P. Campion, C.T. Foxon, B.L. Gallagher, T. Jungwirth, Non-volatile ferroelectric control of ferromagnetism in (Ga, Mn)As, Nat. Mater. 7 (2008) 464–467.
[78] J.M.D. Coey, M. Viret, S. von Molnar, Mixed-valence manganites, Adv. Phys. 48 (1999) 167–293.
[79] X. Hong, A. Posadas, A. Lin A, C. Ahn, Ferroelectric-field-induced tuning of magnetism in the colossal magnetoresistive oxide $La_{1-x}Sr_xMnO_3$, Phys. Rev. B 68 (2003) 133415.
[80] S. Mathews, R. Ramesh, T. Venkatesan, J. Benedetto, Ferroelectric field effect transistor based on epitaxial perovskite heterostructures, Science 276 (1997) 238–240.
[81] T. Kanki, H. Tanaka, T. Kawai, Electric control of room temperature ferromagnetism in a $Pb(Zr_{0.2}Ti_{0.8})O_3/La_{0.85}Ba_{0.15}MnO_3$ field-effect transistor, Appl. Phys. Lett. 89 (2006) 242506.
[82] H. Lu, T.A. George, Y. Wang, I. Ketsman, J.D. Burton, C.-W. Bark, S. Ryu, D.J. Kim, J. Wang, C. Binek, P.A. Dowben, A. Sokolov, C.-B. Eom, E.Y. Tsymbal, A. Gruverman, Electric modulation of magnetization at the $BaTiO_3/La_{0.67}Sr_{0.33}MnO_3$ interfaces, Appl. Phys. Lett. 100 (2012) 232904.
[83] A.F. Vaz, J. Hoffman, Y. Segal, J.W. Reiner, R.D. Grober, Z. Zhang, C.H. Ahn, F.J. Walker, Origin of the magnetoelectric coupling effect in $Pb(Zr_{0.2}Ti_{0.8})O_3/La_{0.8}Sr_{0.2}MnO_3$ multiferroic heterostructures, Phys. Rev. Lett. 104 (2010) 127202.
[84] C.A.F. Vaz, J. Hoffman, Y. Segal, M.S. Marshall, J.W. Reiner, Z. Zhang, R.D. Grober, F.J. Walker, C.H. Ahn, Control of magnetism in $Pb(Zr_{0.2}Ti_{0.8})O_3/La_{0.8}Sr_{0.2}MnO_3$ multiferroic heterostructures, Appl. Phys. 109 (2011) 07D905.
[85] X. Ma, A. Kumar, S. Dussan, H. Zhai, F. Fang, H.B. Zhao, J.F. Scott, R.S. Katiyar, G. Lüpke, Charge control of antiferromagnetism at $PbZr_{0.52}Ti_{0.48}O_3/La_{0.67}Sr_{0.33}MnO_3$ interface, Appl. Phys. Lett. 104 (2014) 132905.
[86] A. Mardana, S. Ducharme, S. Adenwalla, Ferroelectric control of magnetic anisotropy, Nano Lett. 11 (2011) 3862–3867.
[87] E.Y. Tsymbal, H. Kohlstedt, Tunneling across a ferroelectric, Science 313 (2006) 181–183.
[88] E.Y. Tsymbal, A. Gruverman, V. Garcia, M. Bibes, A. Barthélémy, Ferroelectric and multiferroic tunnel junctions, Mater. Res. Soc. Bull. 37 (2012) 138–143.
[89] V. Garcia, M. Bibes, Ferroelectric tunnel junctions for information storage and processing, Nat. Commun. 5 (2014) 4289.
[90] H. Kohlstedt, N. Pertsev, J. Rodríguez Contreras, R. Waser, Theoretical current–voltage characteristics of ferroelectric tunnel junctions, Phys. Rev. B 72 (2005) 125341.
[91] M. Zhuravlev, R. Sabirianov, S. Jaswal, E.Y. Tsymbal, Giant electroresistance in ferroelectric tunnel junctions, Phys. Rev. Lett. 94 (2005) 246802.
[92] V. Garcia, S. Fusil, K. Bouzehouane, S. Enouz-Vedrenne, N.D. Mathur, A. Barthélémy, M. Bibes, Giant tunnel electroresistance for non-destructive readout of ferroelectric states, Nature 460 (2009) 81–84.
[93] A. Gruverman, D. Wu, H. Lu, Y. Wang, H.W. Jang, C.M. Folkman, M.Y. Zhuravlev, D. Felker, M. Rzchowski, C.-B. Eom, E.Y. Tsymbal, Tunneling electroresistance effect in ferroelectric tunnel junctions at the nanoscale, Nano Lett. 9 (2009) 3539–3543.
[94] D. Pantel, S. Goetze, D. Hesse, M. Alexe, Room-temperature ferroelectric resistive switching in ultrathin $Pb(Zr_{0.2}Ti_{0.8})O_3$ films, ACS Nano 5 (2011) 6032–6038.
[95] A. Chanthbouala, A. Crassous, V. Garcia, K. Bouzehouane, S. Fusil, X. Moya, J. Allibe, B. Dlubak, J. Grollier, S. Xavier, C. Deranlot, A. Mostar, R. Proksch, N.D. Mathur, M. Bibes, A. Barthélémy, Solid-state memories based on ferroelectric tunnel junctions, Nat. Nanotechnol. 7 (2012) 101–104.
[96] H. Yamada, V. Garcia, S. Fusil, S. Boyn, M. Marinova, A. Gloter, S. Xavier, J. Grollier, E. Jacquet, C. Carrétéro, C. Deranlot, M. Bibes, A. Barthélémy, Giant electroresistance of super-tetragonal $BiFeO_3$-based ferroelectric tunnel junctions, ACS Nano 7 (2013) 5385–5390.
[97] Z. Wen, C. Li, D. Wu, A. Li, N. Ming, Ferroelectric-field-effect-enhanced electroresistance in metal/ferroelectric/semiconductor tunnel junctions, Nat. Mater. 12 (2013) 617–621.
[98] A. Chanthbouala, V. Garcia, R.O. Cherifi, K. Bouzehouane, S. Fusil, X. Moya, S. Xavier, H. Yamada, C. Deranlot, N.D. Mathur, M. Bibes, A. Barthélémy, J. Grollier, A ferroelectric memristor, Nat. Mater. 11 (2012) 860–864.
[99] D.J. Kim, H. Lu, S. Ryu, C.-W. Bark, C.-B. Eom, E.Y. Tsymbal, A. Gruverman, Ferroelectric tunnel memristor, Nano Lett. 12 (2012) 5697–5702.
[100] D. Pantel, S. Goetze, D. Hesse, M. Alexe, Reversible electrical switching of spin polarization in multiferroic tunnel junctions, Nat. Mater. 11 (2012) 289–293.
[101] V. Garcia, M. Bibes, A. Barthélémy, M. Bowen, E. Jacquet, J.-P. Contour, A. Fert, Temperature dependence of the interfacial spin polarization of $La_{2/3}Sr_{1/3}MnO_3$, Phys. Rev. B 69 (2004) 052403.
[102] J. Nogues, I.K. Schuller, Exchange bias, J. Magn. Magn. Mater. 192 (1999) 203–232.
[103] X. Chen, A. Hochstrat, P. Borisov, W. Kleemann, Magnetoelectric exchange bias systems in spintronics, Appl. Phys. Lett. 89 (2006) 202508.
[104] C. Binek, B. Doudin, Magnetoelectronics with magnetoelectrics, J. Phys. Condens. Matter 17 (2005) L39–L44.
[105] M. Bibes, A. Barthélémy, Towards a magnetoelectric memory, Nat. Mater. 7 (2008) 425–426.
[106] P. Borisov, A. Hochstrat, X. Chen, W. Kleemann, C. Binek, Magnetoelectric switching of exchange bias, Phys. Rev. Lett. 94 (2005) 117203.
[107] A. Hochstrat, Ch. Binek, Xi Chen, W. Kleemann, Extrinsic control of the exchange bias, J. Magn. Magn. Mater. 272–276 (2004) 325–326.
[108] X. He, Y. Wang, N. Wu, A.N. Caruso, E. Vescovo, K.D. Belashchenko, P.A. Dowben, C. Binek, Robust isothermal electric control of exchange bias at room temperature, Nat. Mater. 9 (2010) 579–585.
[109] V. Laukhin, V. Skumryev, X. Marti, D. Hrabovsky, F. Sánchez, M.V. Garcia-Cuenca, C. Ferrater, M. Varela, U. Lüders, J.F. Bobo, J. Fontcuberta, Electric-field control of exchange bias in multiferroic epitaxial heterostructures, Phys. Rev. Lett. 97 (2006) 227201.
[110] M. Fiebig, T. Lottermoser, D. Fröhlich, A.V. Goltsev, R.V. Pisarev, Observation of coupled magnetic and electric domains, Nature 419 (2002) 818.
[111] V. Skumryev, V. Laukhin, I. Fina, X. Martí, F. Sánchez, M. Gospodinov, J. Fontcuberta, Magnetization reversal by electric-field decoupling of magnetic and ferroelectric domain walls in multiferroic-based heterostructures, Phys. Rev. Lett. 106 (2011) 057206.
[112] J. Wang, J.B. Neaton, H. Zheng, V. Nagarajan, S.B. Ogale, B. Liu, D. Viehland, V. Vaithyanathan, D.G. Schlom, U.V. Waghmare, N.A. Spaldin, K.M. Rabe, M. Wuttig, R. Ramesh, Epitaxial $BiFeO_3$ multiferroic thin film heterostructures, Science 299 (2003) 1719–1722.
[113] I. Sosnowska, T. Peterlin-Neumaier, E. Steichele, Spiral magnetic ordering in bismuth ferrite, J. Phys. C, Solid State Phys. 15 (1982) 4835–4846.
[114] F. Bai, J. Wang, M. Wuttig, J. Li, N. Wang, A.P. Pyatakov, A.K. Zvezdin, L.E. Cross, D. Viehland, Destruction of spin cycloid in (111)*c*-oriented $BiFeO_3$ thin films by epitiaxial constraint: enhanced polarization and release of latent magnetization, Appl. Phys. Lett. 86 (2005) 032511.
[115] H. Béa, M. Bibes, S. Petit, J. Kreisel, A. Barthélémy, Structural distortion and magnetism of $BiFeO_3$ epitaxial thin films: a Raman spectroscopy and neutron diffraction study, Philos. Mag. Lett. 87 (2007) 165–174.
[116] T. Zhao, A. Scholl, F. Zavaliche, K. Lee, M. Barry, A. Doran, M.P. Cruz, Y.H. Chu, C. Ederer, N.A. Spaldin, R.R. Das, D.M. Kim, S.H. Baek, C.B. Eom, R. Ramesh, Electrical control of antiferromagnetic domains in multiferroic $BiFeO_3$ films at room temperature, Nat. Mater. 5 (2006) 823–829.
[117] J. Allibe, S. Fusil, K. Bouzehouane, C. Daumont, D. Sando, E. Jacquet, C. Deranlot, M. Bibes, A. Barthélémy, Room temperature electrical manipulation of giant magnetoresistance in spin valves exchange-biased with $BiFeO_3$, Nano Lett. 12 (2012) 1141–1145.

[118] J. Dho, X. Qi, H. Kim, J.L. MacManus-Driscoll, M.G. Blamire, Large electric polarization and exchange bias in multiferroic $BiFeO_3$, Adv. Mater. 18 (2006) 1445–1448.
[119] D. Lebeugle, A. Mougin, M. Viret, D. Colson, L. Ranno, Electric field switching of the magnetic anisotropy of a ferromagnetic layer exchange coupled to the multiferroic compound $BiFeO_3$, Phys. Rev. Lett. 103 (2009) 257601.
[120] Y.H. Chu, L.W. Martin, M.B. Holcomb, M. Gajek, S.J. Han, Q. He, N. Blake, C.H. Yang, D. Lee, W. Hu, Q. Zhan, P.L. Yang, A. Fraile-Rodriguez, A. Scholl, S.X. Wang, R. Ramesh, Electric-field control of local ferromagnetism using a magnetoelectric multiferroic, Nat. Mater. 7 (2008) 478.
[121] J.T. Heron, M. Trassin, K. Ashraf, M. Gajek, Q. He, S.Y. Yang, D.E. Nikonov, Y.H. Chu, S. Salahuddin, R. Ramesh, Electric-field-induced magnetization reversal in a ferromagnet–multiferroic heterostructure, Phys. Rev. Lett. 107 (2011) 217202.
[122] H. Béa, M. Bibes, S. Cherifi, F. Nolting, B. Warot-Fonrose, S. Fusil, G. Herranz, C. Deranlot, E. Jacquet, K. Bouzehouane, A. Barthélémy, Tunnel magnetoresistance and robust room temperature exchange bias with multiferroic $BiFeO_3$ epitaxial thin films, Appl. Phys. Lett. 89 (2006) 242114.
[123] L.W. Martin, Y.-H. Chu, M.B. Holcomb, M. Huijben, P. Yu, S.-J. Han, D. Lee, S.X. Wang, R. Ramesh, Nanoscale control of exchange bias with $BiFeO_3$ thin films, Nano Lett. 8 (2008) 2050–2055.
[124] H. Béa, M. Bibes, F. Ott, B. Dupé, X.-H. Zhu, S. Petit, S. Fusi, C. Deranlot, K. Bouzehouane, A. Barthélémy, Mechanisms of exchange bias with multiferroic $BiFeO_3$ epitaxial thin films, Phys. Rev. Lett. 100 (2008) 017204.
[125] K.L. Livesey, Exchange bias induced by domain walls in $BiFeO_3$, Phys. Rev. B 82 (2010) 064408.
[126] J. Allibe, I.C. Infante, S. Fusil, K. Bouzehouane, E. Jacquet, C. Deranlot, M. Bibes, A. Barthélémy, Coengineering of ferroelectric and exchange bias properties in $BiFeO_3$ based heterostructures, Appl. Phys. Lett. 95 (2009) 182503.
[127] S.M. Wu, S.A. Cybart, P. Yu, M.D. Rossell, J.X. Zhang, R. Ramesh, R.C. Dynes, Reversible electric control of exchange bias in a multiferroic field-effect device, Nat. Mater. 9 (2010) 756–761.
[128] P. Yu, J.-S. Lee, S. Okamoto, M.D. Rossell, M. Huijben, C.-H. Yang, Q. He, J.X. Zhang, S.Y. Yang, M.J. Lee, Q.M. Ramasse, R. Erni, Y.-H. Chu, D.A. Arena, C.-C. Kao, L.W. Martin, R. Ramesh, Interface ferromagnetism and orbital reconstruction in $BiFeO_3/La_{0.7}Sr_{0.3}MnO_3$ heterostructures, Phys. Rev. Lett. 105 (2010) 027201.
[129] M.J. Calderón, S. Liang, R. Yu, J. Salafranca, S. Dong, S. Yunoki, L. Brey, A. Moreo, E. Dagotto, Magnetoelectric coupling at the interface of $BiFeO_3/La_{0.7}Sr_{0.3}MnO_3$ multilayers, Phys. Rev. B 84 (2011) 024422.